

JPET/2002/45328

TITLE PAGE

A KINETIC EVALUATION OF THE ABSORPTION, EFFLUX, AND METABOLISM OF VERAPAMIL IN THE AUTOPERFUSED RAT JEJUNUM

Brendan M. Johnson, Weiqing Chen, Ronald T. Borchardt, William N. Charman, and
Christopher J. H. Porter

Department of Pharmaceutics, Victorian College of Pharmacy – Monash University,
381 Royal Parade, Parkville, Victoria, AUSTRALIA (B.M.J., W.N.C., C.J.H.P.)

Department of Pharmaceutical Chemistry, The University of Kansas, 2095 Constant
Ave, Lawrence, Kansas, USA (W.C.*, R.T.B.)

RUNNING TITLE PAGE

a) Running title: Influence of P-gp and CYP3A on verapamil transport in situ

b) Corresponding author: Dr Christopher J. H. Porter

Dept of Pharmaceutics

Victorian College of Pharmacy

Monash University

381 Royal Pde, Parkville, 3052

Victoria, AUSTRALIA

Ph: +61 3 9903 9649

Fax: + 61 3 9903 9583

Email: Chris.Porter@vcp.monash.edu.au

c) Number of text pages: 23

Number of tables: 4

Number of figures: 4

Number of references: 27

Number of words in *Abstract*: 241

Number of words in *Introduction*: 585

Number of words in *Discussion*: 1259

d) AIC, Akaike Information Criterion; ANOVA, analysis of variance; CV, coefficient of variation; CYP3A, Cytochrome P450 3A; D-519, 5-[(3,4-dimethoxyphenethyl)methylamino]-2-(3,4-dimethoxyphenyl)-valeronitrile; D-617, 2-[3,4-dimethoxyphenyl]-5-methylamino-2-isopropylvaleronitrile; D-620, 5-amino-2-[3,4-dimethoxyphenyl]-2-isopropylvaleronitrile; D-703, 5-[(3,4-dimethoxyphenethyl)methylamino]-2-(4-hydroxy-3-methoxyphenyl)-2-

JPET/2002/45328

isopropylvaleronitrile; ER, extraction ratio; HPLC, high performance liquid chromatography; LOQ, limit of quantitation; MAT, mean absorption time; MRT, mean residence time; MTT, mean transit time; norverapamil, 5-[(3,4-dimethoxyphenethyl)amino]-2-(3,4-dimethoxyphenyl)-2-isopropylvaleronitrile; P-gp, P-glycoprotein; QC, quality control; verapamil, 5-[(3,4-dimethoxyphenethyl)methylamino]-2-(3,4-dimethoxyphenyl)-2-isopropylvaleronitrile.

e) Section assignment: Absorption, Distribution, Metabolism, & Excretion

ABSTRACT

P-glycoprotein (P-gp) mediated drug efflux from the apical membrane of enterocytes is believed to modulate intestinal cytochrome P450 3A (CYP3A) metabolism by altering substrate access to the CYP3A enzyme. This interplay between P-gp and CYP3A was investigated in a rat in situ model of intestinal permeation, where a recirculating luminal perfusion of the jejunum was coupled with mesenteric vein blood collection in order to simultaneously monitor the uptake, transport and metabolism of the P-gp and CYP3A substrate, verapamil. Transport of intact verapamil into the venous blood was increased by 160, 84, and 160%, and the intestinal extraction ratio on passage across the jejunum was reduced by 15, 24, and 97% by inhibitors of P-gp (PSC833), CYP3A (midazolam), or P-gp and CYP3A (ketoconazole), respectively, when present in the luminal perfusate and compared to control experiments. Compartmental kinetic analysis of the data revealed that inhibition of P-gp did not affect the rate constant describing verapamil metabolism, but rather increased the intestinal uptake of verapamil and stimulated a disproportionate increase in verapamil transport into the venous blood. The increase in verapamil transport, in the absence of changes to metabolism, reduced the intestinal extraction ratio. This finding may be explained by saturation of intracellular verapamil binding sites within the intestinal tissue in response to increased verapamil uptake resulting from P-gp inhibition. The current findings confirm previous in vitro and theoretical approaches which suggest that P-gp can modulate the extent of intestinal extraction of P-gp/CYP3A substrates.

Biotransformation of drugs on passage across the enterocyte during oral absorption has been shown to significantly contribute to the first-pass effect of a number of compounds (Thummel et al., 1997). It has further been suggested that the intestinal metabolism of a compound may be increased if that compound is also a substrate for an apically localised efflux transporter, such as P-glycoprotein (P-gp) (Watkins, 1997; Benet and Cummins, 2001; Johnson et al., 2001).

Until recently, the capability of P-gp efflux to increase the enterocyte-based metabolism of a compound has only been rationalised empirically, where it has been suggested that the apical efflux of a compound results in cycles of absorption-efflux-reabsorption, thereby increasing drug exposure to CYP3A. While the simplicity of such an explanation is appealing, a mechanistic basis by which this interaction may occur is not clear, particularly as compounds interacting with P-gp at the apical membrane during absorption are unlikely to have had (as yet) the opportunity to interact with CYP3A (Ambudkar et al., 1999). It is therefore more likely that the net effect of P-gp efflux is an attenuation of the absorption rate of compounds across the apical membrane. Further indirect clinical evidence to support that a reduced absorption rate can impact on intestinal and hepatic extraction is evident in the 20% reduction in the relative oral bioavailability of verapamil after administration of a 240 mg sustained release preparation when compared with an immediate release dosage form, presumably due to increased intestinal and hepatic first-pass extraction (Conway et al., 1990). Similar observations have also been made with propranolol when administered as a sustained release preparation compared with an immediate release dosage form (Wagner, 1985). It is therefore evident, that if P-gp efflux leads to a reduction in drug absorption rate, an increase in the extent of intestinal first-pass

extraction is possible. A mechanism for such an increase in intestinal extraction mediated by P-gp efflux has been proposed (Hochman et al., 2000), and in common with the *in vivo* observations described above, is based on changes to the degree of saturation of drug metabolising enzymes within the enterocyte. It is possible therefore, that P-gp efflux could shift intracellular drug concentrations from the non-linear to the pseudo-linear range for the drug metabolising enzymes. Alternatively, P-gp may act by an as yet unidentified process, such as alterations to saturable drug accumulation or drug distribution patterns within the enterocyte.

To examine the role of P-gp efflux in enterocyte-based drug metabolism more closely, recent studies have examined the impact of a P-gp inhibitor on the extraction ratio of P-gp/CYP3A substrates in transport studies across Caco-2 cell monolayers (Hochman et al., 2000; Cummins et al., 2002), however few studies have examined the interaction between P-gp efflux and CYP3A metabolism *in vivo*. The current studies therefore examined the uptake, transport and metabolism of verapamil in an *in situ* intestinal perfusion model. In this *in situ* model, P-gp inhibition significantly increased the intestinal transport of verapamil and reduced the intestinal extraction ratio of verapamil on passage across the tissue. The impact of both selective and non-selective inhibitors of CYP3A on verapamil metabolism and transport were also examined, and the data codified by the use of a compartmental kinetic model. These data suggest that the impact of PSC833 on the intestinal extraction ratio of verapamil did not result from a direct impact on the rate of CYP3A metabolism, but rather an unidentified indirect event such as saturation of intestinal tissue binding sites and a subsequent increase in verapamil transport into the venous blood.

METHODS

Materials. Verapamil HCl and ketoconazole were supplied by Sigma Chemical Co. (St. Louis, MO). Norverapamil HCl was supplied by Alltech Associates (Baulkham Hills, Australia), D-617, D-620, D-703, and the internal standard D-519, were kind gifts from Knoll AG (Ludwigshafen, Germany). PSC833 was a kind gift from Novartis (Basel, Switzerland) and midazolam was used in the form of a proprietary injection (each 1 ml contained midazolam (as HCl) 5 mg, NaCl 0.8%, disodium edetate 0.01%, benzyl alcohol 1%, adjusted to pH 3.3, Baxter Healthcare Corp, Deerfield, IL). The anaesthetic agents; ketamine (Ketaset, 100 mg.ml⁻¹) and acepromazine (PromAce, 10 mg.ml⁻¹) were supplied by Fort Dodge Animal Health (Fort Dodge, IA); and xylazine (Rompun, 100 mg.ml⁻¹) was obtained from Bayer (Shawnee Mission, KS). All other reagents were analytical grade or higher, all solvents were HPLC grade, and water was obtained from a Labconco water purification system (Kansas City, MO).

Surgical Procedures. All animal studies were performed in accordance with, and approved by, the Institutional Animal Care and Use Committee. The surgical procedures used to prepare the autoperfused rat jejunum with recirculating luminal perfusion are similar to those described elsewhere with slight modifications (Windmueller and Spaeth, 1984; Farraj et al., 1988). Male Sprague-Dawley rats (350-400 g) were anaesthetised by subcutaneous injection (1.5 ml.kg⁻¹) of cocktail I (ketamine, 56 mg.ml⁻¹; xylazine, 15 mg.ml⁻¹; acepromazine, 0.6; mg.ml⁻¹), and subsequent doses (0.44 ml.kg⁻¹) were given hourly with cocktail II (ketamine, 100 mg.ml⁻¹; acepromazine, 1 mg.ml⁻¹). The small intestine was exposed by midline

incision and approximately 15 cm of jejunum was externalised and access to the lumen at the proximal and distal ends of the jejunal segment were made by electrocautery. The segment was then flushed with warm normal saline to remove intestinal contents and cannulated with sections of Teflon tubing (0.03" ID proximal/inlet, Upchurch Scientific, Oak Harbour, WA; and 0.0625" ID distal/outlet, Shimadzu, Kyoto, Japan). The mesenteric vein draining the cannulated jejunal segment was prepared for catheterisation by blunt dissection of the surrounding connective tissue and loose ligatures were placed around extraneous blood vessels perfusing intestinal sections outside the cannulated region. The left jugular vein was then exposed, isolated by blunt dissection, cannulated with silicone tubing (0.012" ID, Helix Medical, Carpinteria, CA), and flushed with heparinised saline (25 U.ml⁻¹). After securing the ligatures around the extraneous blood vessels described above, the animal was heparinised (90 U.kg⁻¹) via the jugular vein cannula, and the mesenteric vein was immediately catheterised with a previously prepared 24G Abbocath-T[®] catheter (Venisystems, Abbott, Ireland), such that after insertion of the catheter and removal of the guide needle, the terminal 1 cm of the outer Teflon catheter remained in the mesenteric vein. Silicone tubing (0.025" ID, 40 cm long, Dow Corning, Midland, MI) was then immediately placed over the exposed catheter tip and the venous blood draining from the cannulated jejunal segment was collected into vials 20 cm below the height of the mesenteric vein. The catheter was secured in place by 3-0 silk suture and infusion of donor blood via the jugular vein cannula was commenced at 0.3 ml.min⁻¹ by peristaltic pump (Amersham Pharmacia Biotech, Piscataway, NJ). Fresh heparinised donor blood (~13 U.ml⁻¹) was collected from donor rats immediately prior to surgery by cardiac puncture.

Luminal Perfusion Protocol. The inlet jejunal cannula was connected to a second peristaltic pump (Amersham Pharmacia Biotech) and perfusate was passed through the lumen at $0.6 \text{ ml} \cdot \text{min}^{-1}$ from a jacketed reservoir that maintained the perfusate at 37°C (Savina et al., 1981). The perfusate contained (in mM): Na^+ , 146.42; K^+ , 4.56; Ca^{2+} , 1.25; Cl^- , 152.06; HPO_4^{2-} , 0.66; H_2PO_4^- , 0.1; adjusted to pH 6.5 at 37°C (Schanker et al., 1958). In experiments other than control, perfusate contained either the P-gp inhibitor PSC833 (20 μM); the CYP3A inhibitor, midazolam (20 μM); or the non-selective P-gp/CYP3A inhibitor ketoconazole (50 μM) (Johnson et al., 2002). Body temperature was maintained by a heating mat and lamp, and the exposed jejunal segment was covered by saline soaked gauze and a clear plastic film. The preparation was allowed to stabilise for 30 min during which time the perfusate exiting the jejunal segment was discarded to waste. After the stabilisation period, the perfusate reservoir was replaced with a reservoir containing a precise volume (10 ml) of 20 μM verapamil in perfusate (with or without appropriate inhibitor). An initial 50 μl sample was taken from the reservoir before commencement of the perfusion through the jejunal segment. After the first 45 sec of perfusion (sufficient to flush the system of buffer once) the outlet cannula was directed to the reservoir to commence the recirculation of the verapamil perfusate. Additional 50 μl and 200 μl samples were taken from the reservoir every 10 min for 1 h. All 50 μl samples were diluted with 150 μl of fresh buffer to bring the concentration of verapamil into the linear range of the HPLC assay, and the undiluted 200 μl samples were used for detection of metabolites (norverapamil, D-617, D-620, and D-703). All perfusate samples were subsequently acidified with 50 μl of 30% acetonitrile in 0.1 M HCl. After the commencement of the verapamil perfusion, mesenteric blood was continuously collected into tared 2 ml tubes at 5 min intervals, weighed, and 500 μl of each blood

sample was transferred to a second 2 ml tube containing 500 μ l of water and 50 μ l of internal standard solution (2.5 μ M D-519). Tubes were briefly vortexed and sonicated to lyse red blood cells, and then stored at -20°C prior to analysis. Correction for blood density was made each day by accurate determination of the mass of blood transferred in the 500 μ l volume delivered by the auto-pipette. At the conclusion of the perfusion experiment (1 h), the animal was sacrificed by injection of a 10 ml air embolus via the jugular vein. The jejunal segment was then flushed with air, removed, dissected longitudinally for accurate determination of surface area, and stored at -20°C for later analysis.

Verapamil and Metabolite Assays. Haemolysed whole blood samples were thawed and vortexed before the addition of 20 μ l of 5 M NaOH and 1 ml of methyl t-butyl ether (EM Science, Gibbstown, NJ). Samples were then vortexed for an additional 5 min before centrifugation at 10000 g for 10 min. The ether layer was then removed by glass pipette to a clean 1.5 ml tube containing 150 μ l of 0.5 M H₂SO₄, vortexed for 2 min, and briefly centrifuged before 100 μ l of the aqueous phase was removed by auto-pipette to an autosampler vial containing 100 μ l of purified water for later HPLC analysis. Intestinal tissue segments were thawed and coarsely cut into pieces with scissors before homogenisation with a Wheaton power Potter-Elvehjem homogeniser in 4 ml of ice cold purified water (Fisher Scientific, Pittsburgh, PA). Duplicate (~500 μ l) portions of homogenate were transferred to tared 2 ml centrifuge tubes containing 50 μ l of internal standard solution (2.5 μ M D-519), weighed, and extracted for verapamil and metabolites as described above. Standard curves for blood and tissue samples were prepared (in duplicate) by the addition of known amounts of verapamil and metabolites (0.0125 to 1 nmol) and 50 μ l of internal standard solution to blank

JPET/2002/45328

blood and jejunal homogenate (500 μ l), and were extracted at the same time as their corresponding samples by the method described above. High range (0.02 to 5 μ M) and low range (0.02 to 1 μ M) standard curves for verapamil and metabolites, respectively, were prepared in blank perfusate, by the addition of 50 μ l of concentrated standard (prepared in 30% acetonitrile in 0.1 M HCl) to 200 μ l of blank perfusate.

Acidified perfusate, extracted blood, extracted tissue samples and all corresponding standards were analysed for verapamil, norverapamil, D-617, D-620, D-703, and D-519 by a gradient HPLC method. The HPLC consisted of Shimadzu SIL-10A autosampler and SCL-10A controller, two LC-6A pumps and SCL-6A controller, and an RF-535 fluorescence monitor with excitation and emission wavelengths set to 280 and 310 nm respectively (Shimadzu, Kyoto, Japan). A 100 μ l portion of sample was injected onto an Xterra MS C₁₈ 5 μ M 3.9 \times 150 mm column (Waters, Milford, MA) and mobile phase was delivered at 1 ml.min⁻¹. Mobile phase A consisted of 90% 5 mM ammonium acetate (pH 4.2) with 10% acetonitrile, and mobile phase B was 100% acetonitrile. The initial proportion of mobile phase B was 13% which was increased to 15% over 3 min, further increased to 24% over another 10 min, subsequently held at 24% for 3 min, before being increased to 40% over 4 min and finally held at 40% for a further 1 min, before returning to 13% over 1 min. The proportion of mobile phase B was then held at 13% to provide a 4 min re-equilibration period.

JPET/2002/45328

Perfusate, whole blood, and tissue homogenate assays for verapamil and metabolites were validated with quadruplicate quality control (QC) standards on 4 separate occasions. The perfusate assay was validated using high (5 μM), medium (1 μM), and low (0.1 μM) concentration QC standards of verapamil, and medium (1 μM) and low (0.1 μM) concentration QC standards for the metabolites. Perfusate assay accuracy (for all analytes) was within 5% of target concentration. Precision, as measured by the coefficient of variation (CV), for all compounds was less than 5%, and the interday variation in precision and accuracy was less than 5%. The LOQ (limit of quantitation) for all compounds was set at 0.02 μM where accuracy was within 10% of target and CV <15%. The whole blood assay was validated using high (1 μM) and low (0.1 μM) QC standards for verapamil and metabolites in 500 μl of whole blood where accuracy was within 5% of target (except for D-620 which was within 9%), and precision CV was less than 10%. The interday variation was less than 8% and the LOQ for all compounds was set at 0.025 μM where the accuracy (for all analytes) was within 10% of target and the CV was <20%. The mean extraction efficiency for verapamil, norverapamil, D-617, D-620, and D-703 from whole blood samples was 96, 97, 86, 70, and 94%, respectively. The tissue homogenate assay was validated using high (0.5 nmol) and low (0.05 nmol) QC quantities of verapamil and metabolites in 500 μl of blank tissue homogenate. The mean accuracy for all compounds was within 10% of target and the precision CV was less than 10%. The interday variation was <5% and the LOQ was set at 0.0125 nmol per 500 μl of homogenate where for all analytes the accuracy was within 10% of target and the precision CV was <20%. The mean extraction efficiency for verapamil, norverapamil, D-617, D-620, and D-703 from tissue homogenate was 96, 96, 78, 72, and 84%, respectively.

Data Analysis. In validation experiments, non-specific adsorption of verapamil to the perfusion apparatus was observed and virtually complete after 10 min (approximately 10% of verapamil dose). Therefore, the 10 min perfusate sample was designated t=0 and all presented data and calculations hereafter have been made relative to this time point. Total mass balance (% recovery) of verapamil and metabolites across the entire preparation in control, PSC833, midazolam, and ketoconazole experiments, were 97 ± 8 , 87 ± 5 , 93 ± 5 , and 95 ± 7 %, respectively (mean \pm SD, n=4-7 determinations). The net flux of water from the perfusate across the jejunum ($23 \pm 51 \mu\text{l} \cdot \text{cm}^{-2}$ over 60 min, mean \pm SD, n=10) and the adhered water volume to the intestinal tissue ($25 \pm 7 \mu\text{l} \cdot \text{cm}^{-2}$, mean \pm SD, n=10) were determined in sham validation experiments conducted with [^{14}C]-PEG 4000 in the luminal perfusate. Correction factors based on these data were subsequently applied to verapamil in situ perfusion data where appropriate.

The apparent permeability coefficient of verapamil calculated from its appearance in venous blood was calculated using Equation 1 (Martin, 1993), where dX/dt is the rate of verapamil appearance in venous blood ($\text{nmol} \cdot \text{sec}^{-1}$), A is the surface area of the jejunal segment (cm^2), and C_0 is the concentration of verapamil in the perfusate at time 10 min ($\text{nmol} \cdot \text{cm}^{-3}$).

$$\text{Appearance permeability (cm} \cdot \text{sec}^{-1}) = \frac{dX/dt}{A \cdot C_0} \quad \text{Equation 1}$$

The apparent permeability coefficient of verapamil calculated from its disappearance from the luminal perfusate was calculated by Equation 2 (Ho et al., 1977), where the uptake rate constant, k_u (sec^{-1}), was calculated from the negative slope of a \log_e perfusate concentration versus time plot and V is the volume of the perfusate (cm^3).

$$\text{Disappearance permeability (cm.sec}^{-1}\text{)} = \frac{V}{A} \cdot k_u \quad \text{Equation 2}$$

The extraction ratio (ER) of verapamil on passage through the jejunal tissue was calculated using Equation 3 (Cummins et al., 2001) and Equation 4 (Fisher et al., 1999) at the conclusion of experiments when accurate determinations of tissue bound parent and metabolite were made, where the subscripts p , b and t represent the total amount (nmol) of metabolite or parent compound in the perfusate, blood, and tissue segment, respectively.

$$\text{Cummins ER} = \frac{\sum \text{METABOLITE}_{p,b,t}}{\sum \text{METABOLITE}_{p,b,t} + \sum \text{PARENT}_{b,t}} \quad \text{Equation 3}$$

$$\text{Fisher ER} = \frac{\sum \text{METABOLITE}_{p,b,t}}{\sum \text{METABOLITE}_{p,b,t} \sum \text{PARENT}_b} \quad \text{Equation 4}$$

Compartmental Modelling. Compartmental kinetic modelling of the in situ perfusion data was performed using ordinary least squares regression and the Levenberg-Marquardt fitting algorithm with 4th order Runge-Kutta integration (ModelMaker 4.0, Modelkinetix, UK). In the interests of parsimony, the individual levels of metabolites detected (norverapamil, D-617, and D-620) in perfusate, tissue and blood samples, respectively, have been pooled and referred to as “metabolite(s)”. In order to adequately fit a closed compartmental model to the perfusion data, correction for any discrepancy in mass balance must be made, therefore data in each compartment was adjusted proportionally to achieve a mass balance of 100%, requiring adjustment of no more than 13%. The luminal surface area available for diffusion was also standardised to 15 cm². The model shown in Fig. 1 was simultaneously fitted to data from each individual experiment for each data set (control, PSC833, midazolam or ketoconazole), where all rate constants were

assumed to be first order and all compartments well-stirred. Higher order models, such as the inclusion of a k_{2l} parameter or Michaelis-Menten metabolism kinetics, were poorly estimated and did not significantly improve the model as measured by the AIC and a non-significant F ratio test. A model predicted ER was determined by Equation 5, which estimates the ER based on the compartmental model in Fig. 1 (Rowland et al., 1973).

$$\text{Model Predicted ER} = \frac{k_{20}}{k_{20} + k_{23}} \quad \text{Equation 5}$$

Mean time parameters (in min) were determined by Equations 6 through 8, where the MAT, MTT, and MRT are the mean absorption time, mean transit time, and mean residence time, respectively (Veng-Pedersen, 1989; Lee and Amidon, 1996).

$$\text{MAT} = \frac{1}{k_{12}} \quad \text{Equation 6}$$

$$\text{MTT} = \frac{1}{k_{20} + k_{23}} \quad \text{Equation 7}$$

$$\text{MRT} = \text{MAT} + \text{MTT} \quad \text{Equation 8}$$

Statistical Analysis. Comparisons between apparent permeability coefficients, tissue bound verapamil or metabolite, and extraction ratios across data sets were made by one-way analysis of variance with post-hoc multiple pair-wise comparisons (Student-Newman-Keuls test). Validity, accuracy and precision of the compartmental models were assessed by examination of the standardised residuals, %CV of the parameter estimates, r^2 , and significance (p value) of the F ratio. Comparisons between control and PSC833, midazolam, or ketoconazole estimated rate constants were made by Student's t test where $p < 0.05$ was considered significant (Boxenbaum et al., 1974; Landaw and DiStefano III, 1984).

RESULTS

Verapamil Permeability in the Autoperfused Rat Jejunum. Apparent permeability coefficients of verapamil calculated from verapamil appearance in venous blood and disappearance from the luminal perfusate in the in situ autoperfused rat jejunum are shown in Table 1, and mass balance corrected absorption and metabolism profiles are shown in Fig. 2. The appearance of verapamil in venous blood was significantly increased by P-gp inhibition (via PSC833), CYP3A inhibition (via midazolam), or inhibition of both P-gp and CYP3A (via ketoconazole); by 160, 84, and 160%, respectively. The disappearance of verapamil from the luminal perfusate was not significantly altered by the inhibitors, however, the disappearance permeability coefficients of verapamil (in the presence and absence of any inhibitor) were considerably higher (2.7 to 7.7-fold) than those based on verapamil appearance in the venous blood. The disappearance and appearance permeability coefficients of the passive transcellular (antipyrine), and paracellular (mannitol) markers were unaffected by the addition of 20 μ M PSC833, 20 μ M midazolam, or 50 μ M ketoconazole to the luminal perfusate (data not shown).

Appearance of Verapamil Metabolites in the Autoperfused Rat Jejunum. The two major metabolites of verapamil detected in the current studies were the CYP3A mediated N-dealkylated and N-demethylated products, D-617 and norverapamil, respectively. Each metabolite was formed in similar quantities in the current in situ study, which is consistent with our previous in vitro findings (Johnson et al., 2001). In a number of studies, N-(dealkyldemethyl)-verapamil (D-620), was also observed in perfusate samples at approximately 10% of the molar concentration of D-617 and

norverapamil. For ease of data presentation, all individual metabolites have been pooled and are referred to as “metabolite”. After a slight lag phase, the formation of metabolite was essentially linear with respect to time, and in control experiments, the amount of metabolite secreted back into the luminal perfusate was significantly higher than the amount of intact verapamil appearing in the venous blood (Fig. 2). Metabolite appearance was significantly reduced by CYP3A inhibition (midazolam or ketoconazole, Fig. 2). The P-gp inhibitor, PSC833, while not significantly altering the amount of metabolite secreted back into the luminal perfusate, considerably increased the amount of metabolite appearing in the venous blood. This is consistent with P-gp inhibition leading to increased verapamil uptake and increased metabolite formation.

Accumulation of Verapamil and Metabolites in Jejunal Tissue. The accumulation of verapamil and metabolite within the tissue segment at the conclusion of transport experiments is shown in Fig. 2. The time course of accumulation of verapamil and metabolite in the tissue was generated from the difference between disappearance from the luminal perfusate and appearance in the venous blood and assuming mass balance across the system. Mass balance was proven in pre-study validation and the verapamil and metabolite mass present in the tissue at the end of the experiment was confirmed by assay. The tissue accumulation of verapamil was not significantly altered by the presence of the inhibitors PSC833, midazolam, or ketoconazole. However, the amount of metabolite detected in the tissue was significantly increased by PSC833, consistent with increased metabolism of verapamil (due to increased verapamil uptake resulting from P-gp inhibition) and reduced efflux of the

metabolites. Tissue levels of metabolite were also significantly reduced by ketoconazole (CYP3A inhibition).

Extraction Ratio of Verapamil. The extraction ratios (ER) of verapamil in the presence and absence of the inhibitors PSC833, midazolam, and ketoconazole on passage across the rat jejunum were determined by Equations 3 and 4 and are shown in Table 2. As both calculations require the amount of intracellular metabolite and/or parent compound to be known, these calculations were only applied to data collected at the terminal time point (i.e., when the intestinal tissue was homogenised and assayed for metabolites and verapamil). The ER was 0.45 ± 0.11 under control conditions when calculated by Equation 3 from Cummins et al (2001). The Cummins ER was not significantly reduced by the P-gp inhibitor, PSC833, but as expected, was significantly reduced by CYP3A inhibition (midazolam or ketoconazole). In contrast, when the ER was calculated using Equation 4 described by Fisher et al (1999), where the amount of parent compound in the intestinal tissue segment is neglected, the ER was 0.75 ± 0.06 and was significantly reduced by PSC833, midazolam, and ketoconazole, by 15, 24, and 97%, respectively. Interestingly, the model predicted ER, calculated from the first order rate constants estimated from compartmental kinetic analysis of the perfusion data (Equation 5), was in excellent agreement with the Fisher ER. The model predicted ER of the ketoconazole group, however, was estimated with less accuracy as a result of the very low levels of metabolite produced leading to poor estimation of the k_{20} parameter (CV of 63%).

Model Fitting. The compartmental model described in Fig. 1 was simultaneously fitted to data from each individual experiment from control, PSC833, midazolam, and

ketoconazole data sets. Parameter estimates and goodness-of-fit statistics are shown in Table 3, and the model predicted data for each experimental group are plotted against the observed data in Fig. 2. Excellent agreement between observed and predicted data is evident, and the parameters describing the disposition of verapamil in the experimental system are precisely estimated (low %CV, Table 3). Parameters describing the distribution of metabolite were estimated with less precision, particularly for the ketoconazole data set (due to the extremely low levels of metabolite observed). The rate constant k_{12} in this model represents the net influx of verapamil into the enterocyte, and higher order models, such as the inclusion of a k_{21} parameter to discretely define P-gp mediated efflux, and the replacement of k_{20} with a Michaelis-Menten function, were not statistically better models to that described in Fig. 1 as evidenced by non-significant changes in the residual sum of squares, and poor estimation (high %CV) of these additional parameters (data not shown).

Rate Constant Analysis. Statistical analysis of the rate constants describing verapamil transport revealed that k_{12} , the rate constant encompassing verapamil uptake into the enterocyte, was significantly increased by PSC833, consistent with inhibition of the apically localised P-gp efflux process. The parameter describing the first order metabolism of verapamil, k_{20} , was significantly reduced by the CYP3A inhibitors, midazolam and ketoconazole, but unaffected by the selective P-gp inhibitor PSC833. Interestingly, k_{23} , the parameter describing the first order transport of verapamil from the enterocyte to the venous blood was significantly increased by all inhibitors. PSC833 also reduced the k'_{01} parameter (although the low precision of estimation precluded attainment of statistical significance). The lowered k'_{01}

parameter reflects reduced transport of metabolite from the tissue to the luminal perfusate and is consistent with inhibition of P-gp mediated efflux of the metabolites.

Mean Time Parameters. The mean absorption time (MAT), or the mean time taken for luminal verapamil to be completely absorbed from the lumen was dramatically reduced by PSC833, but generally unaffected by midazolam or ketoconazole (Table 4). The mean transit time (MTT), or the average time spent by verapamil in the intestinal tissue before being either metabolised or transported to the venous blood, was slightly (but not significantly) increased by midazolam, but significantly increased by ketoconazole. The impact of ketoconazole on MTT is consistent with metabolic inhibition increasing the longevity of a molecule in the enterocyte via a reduction in metabolic clearance. The mean residence time (MRT) is an additive property of the MAT and MTT, and is a reflection of the average time taken for a verapamil molecule to move from the luminal perfusate to the venous blood. The MRT of verapamil in this model was only significantly reduced by PSC833. In the presence of ketoconazole, the increased MTT (CYP3A inhibition) is counter to the slightly reduced MAT (P-gp inhibition); therefore no significant change in MRT is evident.

DISCUSSION

The uptake and transport of verapamil in the autoperfused rat jejunum was monitored by determination of permeability coefficients based on verapamil disappearance from the luminal perfusate and appearance in venous blood, respectively. P-gp inhibition by PSC833 resulted in a significant increase in verapamil appearance into the venous blood in the current experimental system, consistent with reduced P-gp efflux resulting in increased verapamil absorption and transport across the enterocyte. Similar to the observations made in the presence of PSC833, inhibition of intestinal CYP3A metabolism by midazolam increased the transport of verapamil into venous blood, presumably as a result of reduced metabolic clearance, and ketoconazole further increased verapamil transport when compared to midazolam due to the dual inhibition of both CYP3A and P-gp (Table 1, Fig. 2). Interestingly, none of the inhibitors employed in the current studies significantly altered the disappearance of verapamil from the luminal perfusate (Table 1). This finding is in agreement with previous *in vivo* observations with verapamil (Sandström et al., 1999), and most likely reflects the small impact of P-gp efflux on the disappearance of verapamil from the luminal perfusate relative to the high intrinsic permeability and substantial tissue uptake of verapamil. These data also illustrate the potentially different conclusions that may be drawn as to the importance of P-gp efflux on drug absorption when assessing permeability on drug disappearance as opposed to drug appearance data.

The current experimental preparation (consisting of perfusate, tissue, and blood sampling sites), was most simply described by a 3 compartment system (Fig. 1). This model effectively described the uptake, metabolism and transport of verapamil and

metabolite and the parameters (rate constants) describing the disposition of verapamil were accurately and precisely estimated (Fig. 2 and Table 3). The development of the compartmental model in the current studies also allows for a theoretical assessment of the interplay between P-gp efflux and high intrinsic passive permeability, such as that displayed (at least when using disappearance permeability) by verapamil in the current in situ preparation, and in previous in vitro and in vivo studies (Sandström et al., 1999; Polli et al., 2001). The possible impact of high passive permeability on efflux kinetics is illustrated in Fig. 3, where the % increase in drug transport expected after complete inhibition of P-gp efflux is simulated with respect to variation in the passive influx of verapamil and the maximum rate of P-gp mediated efflux (V_{max}). These simulations demonstrate that the increase in drug transport expected on P-gp inhibition will be greatest for compounds with inherently lower influx rates (which can result from low intrinsic permeability of the compound, or similarly, from a low dose of a high intrinsic permeability compound) and/or compounds with higher V_{max} , and are consistent with previous studies in the literature (Eytan et al., 1997; Döppenschmitt et al., 1999).

A further aim of the current studies was to assess the impact of P-gp efflux on the extent of intestinal drug metabolism, and this can most clearly be examined by determination of the intestinal extraction ratio (ER) of verapamil under control conditions and in the presence of selective P-gp inhibition (PSC833). Under conditions where tissue accumulation of parent compound has not reached steady-state, two previously suggested methods may be used for determination of the intestinal ER, Equation 3 from Cummins et al (2001) and Equation 4 from Fisher et al (1999). These two methods of calculation differ only by the inclusion of the quantity

of intracellular parent compound in the denominator of Equation 3. Regardless of the method of calculation, the ER of verapamil was, as expected, significantly reduced by CYP3A inhibition, i.e., in the presence of midazolam or ketoconazole. In the current in situ studies, P-gp inhibition by PSC833 only led to significant reduction in the ER of verapamil when calculated by the method of Fisher et al (1999). If the model described in Fig. 1 is assumed (and the ER is calculated from predicted data using Equations 3 and 4), it is apparent that the Fisher ER is constant with respect to time, and is equal to the model predicted ER that can be calculated using Equation 5 (Fig. 4 and Table 2). In contrast, the Cummins ER gradually increases with time and asymptotically approaches the value of the predicted Fisher ER as time approaches infinity, i.e., when the intracellular drug mass approaches zero and absorption is virtually complete (Fig. 4). Since the value of the Cummins ER is dependent on the extent of drug uptake in the tissue, the ER is dependent on the time at which it is determined (Cummins et al., 2002). The Fisher ER however is not time-dependent, and predicts the extraction ratio at the completion of absorption. Therefore, the inability to observe a significant difference in the Cummins ER in the presence and absence of P-gp inhibition (PSC833) in the current studies most likely reflects variation in the relatively large amounts intracellular verapamil present. However, as drug absorption approaches completion, and intracellular drug levels fall, a significant difference in the ER in the presence of PSC833 is expected to be revealed, and is apparent when examined using Equations 4 or 5.

Analysis of the rate constants describing the model in Fig. 1 revealed that while PSC833 increased the uptake of verapamil in this model (increased k_{12} compared to control), a proportional increase in the extent of verapamil metabolism was also

observed between control and PSC833 groups (insignificant difference in k_{20}). Therefore, despite more rapid verapamil uptake in the presence of P-gp inhibition (reduced MAT), it appears that linear metabolism was maintained. However, all of the inhibitors employed in the current studies increased the transport of verapamil from the intestinal tissue into the venous blood when compared to control. This kinetic evidence therefore suggests that the reduction in ER evident on inhibition of P-gp was not due to a reduction in metabolism or saturation of the CYP3A enzyme itself (as k_{20} was unaltered in the presence of PSC833); but rather resulted from a disproportionate increase in transport *out* of the cell into the venous blood (increased k_{23}). The increase in k_{23} observed in the presence of PSC833 implies that P-gp inhibition may have ramifications beyond increased absorption rate across the apical membrane and may indirectly result in increased drug transport across the absorptive barrier. Therefore, whilst the model used in the current study is entirely linear in nature, this disproportionate (or non-linear) change in the rate of drug transport to the venous blood (increase in the *rate constant* k_{23}) provides for a non-linear relationship between the extent of drug metabolism and the extent of drug transport, thereby allowing PSC833 (P-gp inhibition) to reduce the ER. Although the mechanism underlying this increase in transport is not clear, the current data could be explained by saturation of intracellular drug binding sites, such that increases in intracellular drug concentration, eg, via P-gp (or CYP3A) inhibition, are reflected in disproportionate increases in drug transport out of the tissue into venous blood.

In summary, the permeability of verapamil across the autoperfused rat jejunum *in situ* was significantly increased by P-gp or CYP3A inhibition. The P-gp inhibitor, PSC833, reduced P-gp mediated efflux of verapamil, and the extraction ratio of

JPET/2002/45328

verapamil across the rat intestinal tissue was significantly reduced by P-gp and/or CYP3A inhibition. Additionally, the reduction in ER observed in the presence of the P-gp inhibitor PSC833 appeared not to result from a reduction in the rate of metabolite formation, but rather, via a disproportionate increase in drug transport into the mesenteric blood, an effect that may be secondary to saturable intestinal tissue binding of verapamil.

ACKNOWLEDGEMENTS

The authors gratefully acknowledge the generosity of Knoll AG for supply of the verapamil metabolite panel and internal standard, Novartis for the supply of the P-gp inhibitor PSC833, and Dr Elizabeth Topp (University of Kansas) and Dr Roger Nation (Monash University) for useful discussions regarding the theoretical models.

REFERENCES

- Ambudkar SV, Dey S, Hrycyna CA, Ramachandra M, Pastan I and Gottesman MM (1999) Biochemical, cellular, and pharmacological aspects of the multidrug transporter. *Annu Rev Pharmacol Toxicol* **39**:361-398.
- Benet LZ and Cummins CL (2001) The drug efflux-metabolism alliance: biochemical aspects. *Adv Drug Deliv Rev* **50**:S3-S11.
- Boxenbaum HG, Riegelman S and Elashoff RM (1974) Statistical estimations in pharmacokinetics. *J Pharmacokinet Biopharm* **2**:123-148.
- Conway EL, Phillips PA, Drummer OH and Louis WJ (1990) Influence of food on the bioavailability of a sustained-release verapamil preparation. *J Pharm Sci* **79**:228-231.
- Cummins CL, Jacobsen W and Benet LZ (2002) Unmasking the dynamic interplay between intestinal P-glycoprotein and CYP3A4. *J Pharmacol Exp Ther* **300**:1036-1045.
- Cummins CL, Mangravite LM and Benet LZ (2001) Characterizing the expression of CYP3A4 and efflux transporters (P-gp, MRP1, and MRP2) in CYP3A4-transfected Caco-2 cells after induction with sodium butyrate and the phorbol ester 12-O-tetradecanoylphorbol-13-acetate. *Pharm Res* **18**:1102-1109.
- Döppenschmitt S, Spahn-Langguth H, Regårdh CG and Langguth P (1999) Role of P-glycoprotein-mediated secretion in absorptive drug permeability: an approach using passive membrane permeability and affinity to P-glycoprotein. *J Pharm Sci* **88**:1067-1072.
- Eytan GD, Regev R, Oren G, Hurwitz CD and Assaraf YG (1997) Efficiency of P-glycoprotein-mediated exclusion of rhodamine dyes from multidrug-resistant

cells is determined by their passive transmembrane movement rate. *Eur J Biochem* **248**:104-112.

Farraj NF, Davis SS, Parr GD and Stevens HNE (1988) Absorption of progabide from aqueous solutions in a modified recirculating rat intestinal perfusion system. *Int J Pharm* **43**:93-100.

Fisher JM, Wrighton SA, Watkins PB, Schmiedlin-Ren P, Calamia JC, Shen DD, Kunze KL and Thummel KE (1999) First-pass midazolam metabolism catalyzed by 1 α ,25-dihydroxy vitamin D₃-modified Caco-2 cell monolayers. *J Pharmacol Exp Ther* **289**:1134-1142.

Ho NFH, Park JY, Morozowich W and Higuchi WI (1977) Physical model approach to the design of drugs with improved intestinal absorption, in *Design of Biopharmaceutical Properties through Prodrugs and Analogs* (Roche EB ed) pp 136-227, American Pharmaceutical Association Academy of Pharmaceutical Sciences, Washington.

Hochman JH, Chiba M, Nishime J, Yamazaki M and Lin JH (2000) Influence of P-glycoprotein on the transport and metabolism of indinavir in Caco-2 cells expressing cytochrome P-450 3A4. *J Pharmacol Exp Ther* **292**:310-318.

Johnson BM, Charman WN and Porter CJH (2001) The impact of P-glycoprotein efflux on enterocyte residence time and enterocyte-based metabolism of verapamil. *J Pharm Pharmacol* **53**:1611-1619.

Johnson BM, Charman WN and Porter CJH (2002) An in vitro examination of the impact of PEG 400, Pluronic P85, and Vitamin E TPGS on P-glycoprotein efflux and enterocyte-based metabolism in excised rat intestine. *AAPS PharmSci* **4**:article 40.

- Landaw EM and DiStefano III JJ (1984) Multiexponential, multicompartmental, and noncompartmental modeling. II. Data analysis and statistical considerations. *Am J Physiol* **246**:R665-677.
- Lee PID and Amidon GL (1996) *Pharmacokinetic Analysis: A Practical Approach*. Technomic Publishing Co., Lancaster.
- Martin A (1993) *Physical Pharmacy: Physical Chemical Principles in the Pharmaceutical Sciences*. Lippincott Williams and Wilkins, Baltimore.
- Polli JW, Wring SA, Humphreys JE, Huang LY, Morgan JB, Webster LO and Serabjit-Singh CS (2001) Rational use of in vitro P-glycoprotein assays in drug discovery. *J Pharmacol Exp Ther* **299**:620-628.
- Rowland M, Benet LZ and Graham GG (1973) Clearance concepts in pharmacokinetics. *J Pharmacokinet Biopharm* **1**:123-136.
- Sandström R, Knutson TW, Knutson L, Jansson B and Lennernäs H (1999) The effect of ketoconazole on the jejunal permeability and CYP3A metabolism of (R/S)-verapamil in humans. *Br J Clin Pharmacol* **48**:180-189.
- Savina PM, Staubus AE, Gaginella TS and Smith DF (1981) Optimal perfusion rate determined for in situ intestinal absorption studies in rats. *J Pharm Sci* **70**:239-243.
- Schanker LS, Tocco DJ, Brodie BB and Hogben CAM (1958) Absorption of drugs from the rat small intestine. *J Pharmacol Exp Ther* **123**:81-88.
- Thummel KE, Kunze KL and Shen DD (1997) Enzyme-catalyzed processes of first-pass hepatic and intestinal drug extraction. *Adv Drug Deliv Rev* **27**:99-127.
- Veng-Pedersen P (1989) Mean time parameters in pharmacokinetics. Definition, computation and clinical implications (Part I). *Clin Pharmacokinet* **17**:345-366.

JPET/2002/45328

Wagner JG (1985) Propranolol: pooled Michaelis-Menten parameters and the effect of input rate on bioavailability. *Clin Pharmacol Ther* **37**:481-487.

Watkins PB (1997) The barrier function of CYP3A4 and P-glycoprotein in the small bowel. *Adv Drug Deliv Rev* **27**:161-170.

Windmueller HG and Spaeth AE (1984) Vascular perfusion of rat small intestine for permeation and metabolism studies, in *Pharmacology of Intestinal Permeation* (Csáky TZ ed) pp 113-156, Springer-Verlag, Berlin.

FOOTNOTES

a) Financial support for B.M.J. was provided by an Australian Postgraduate Award (Monash University) and a Globalization of Pharmaceuticals Education Network (GPEN) travel grant.

b) Reprint requests can be sent to: Dr Christopher J. H. Porter

Dept of Pharmaceutics

Victorian College of Pharmacy

Monash University

381 Royal Pde, Parkville, 3052

Victoria, AUSTRALIA

JPET/2002/45328

TABLE 1

Apparent permeability coefficients ($\times 10^6$ cm.sec⁻¹) of verapamil (20 μ M) calculated from appearance in venous blood and disappearance from the luminal perfusate in the presence and absence of 20 μ M PSC833, 20 μ M midazolam, or 50 μ M ketoconazole conducted in the autoperfused rat jejunum with recirculating luminal perfusion.

Data represents the mean \pm SD of n=4-7 determinations.

	Appearance			Disappearance		
control	3.96	\pm	1.28	30.66	\pm	10.76
PSC833	10.40	\pm	3.23*	38.37	\pm	7.08
midazolam	7.30	\pm	0.90*	26.66	\pm	3.71
ketoconazole	10.32	\pm	1.94*	28.21	\pm	2.84

*Significant difference compared to control permeability (p<0.025)

JPET/2002/45328

TABLE 2

Observed and predicted extraction ratios (ER) of verapamil on transport across the in situ autoperfused rat jejunum in the presence and absence of 20 μ M PSC833, 20 μ M midazolam, or 50 μ M ketoconazole

Cummins, Fisher, and model predicted extraction ratios of verapamil were calculated with Equations 3, 4, and 5, respectively. Observed data is the mean and SD of n=4-7 determinations.

	Cummins ER	Fisher ER	model predicted ER
control	0.45 \pm 0.11	0.75 \pm 0.06	0.77
PSC833	0.42 \pm 0.07	0.64 \pm 0.07*	0.65
midazolam	0.33 \pm 0.06*	0.57 \pm 0.10*	0.59
ketoconazole	0.01 \pm 0.01*	0.02 \pm 0.02*	0.17

*Significantly different to respective control ER (p<0.05)

JPET/2002/45328

TABLE 3

Parameter estimates (k_{ij} , min⁻¹) and goodness-of-fit statistics for the model described in Fig. 1 fitted to control, PSC833, midazolam, and ketoconazole data sets from in situ perfusion experiments in the autoperfused rat jejunum.

Models were fitted using ordinary least squares regression and the model predicted data are shown in Fig. 2.

parameter	control		PSC833		midazolam		ketoconazole	
	estimate	%CV	estimate	%CV	estimate	%CV	estimate	%CV
k_{12}	0.0027	3	0.0045*	2	0.0030	2	0.0029	3
k_{23}	0.0113	22	0.0186*	11	0.0175*	9	0.0179*	8
k_{20}	0.0380	17	0.0341	13	0.0248*	13	0.0036*	63
k'_{01}	0.1141	39	0.0518	24	0.1079	34	0.0275	180
k'_{03}	0.0156	76	0.0230	32	0.0155	68	0.0156	240
F ratio	26858		18302		50562		37654	
p value	<0.001		<0.001		<0.005		<0.005	
r^2	0.9977		0.9971		0.9993		0.9991	

*Significantly different to the corresponding control parameter (p<0.05)

JPET/2002/45328

TABLE 4

Mean time parameters (mean absorption time, MAT; mean transit time, MTT; and mean residence time, MRT), in min, of verapamil in the autoperfused rat jejunum from control, PSC833, midazolam, and ketoconazole compartmental models

Parameters were calculated based on the compartmental model in Fig. 1 and the rate constants shown in Table 3.

	MAT (%CV)	MTT (%CV)	MRT (%CV)
control	374 (3)	20 (14)	394 (3)
PSC833	223 (2)*	19 (9)	242 (2)*
midazolam	338 (2)	24 (8)	361 (2)
ketoconazole	349 (3)	46 (12)*	395 (3)

*Significantly different to all other groups (p<0.001)

Fig. 1. Compartmental model fitted to control, PSC833, midazolam, and ketoconazole data sets, where all rate constants were assumed to be first order and all compartments well-stirred. Compartments 1, 2, and 3 represent the disposition of verapamil in the perfusate, intestinal tissue, and venous blood, respectively, and compartments 1', 0, and 3' represent the total amount of metabolite in the perfusate, intestinal tissue, and venous blood, respectively.

Fig. 2. Observed (symbols) and predicted (full and dotted lines) data from verapamil (20 μ M) permeability studies in the in situ autoperfused rat jejunum with recirculating luminal perfusion, in the absence (control), and presence of 20 μ M PSC833, 20 μ M midazolam, or 50 μ M ketoconazole, in the luminal perfusate, where verapamil (●,—) and metabolite (○,.....) are presented as % of the initial verapamil dose, in the luminal perfusate (Panel A), venous blood (Panel B), and intestinal tissue (Panel C).

Fig. 3. Predicted increase in drug transport on complete inhibition of P-gp after a 50 min transport study on variation of passive influx permeability and V_{max} of P-gp secretory efflux. Data were generated after simulation studies with the model described in Fig. 1 and parameter estimates generated from control verapamil experiments after inclusion of a saturable P-gp efflux expression in the transfer of drug from compartment 1 to 2, such that the differential equation describing drug disposition in compartment 1 was rewritten as:

$$dX_1/dt = k_{12} \cdot X_1 - V_{max} \cdot X_2 / (K_m + X_2),$$

where: X_1 and X_2 represent the amount (%) of drug in compartments 1 and 2, respectively; the K_m of P-gp efflux was arbitrarily set to 1 %; and the V_{max} was varied between 0.1 and 0.5 %. min^{-1} .

Fig. 4. Simulated extraction ratios of verapamil with respect to time in the absence (control) and presence of P-gp inhibition (PSC833) generated from numerical integration of the model described in Fig. 1 using the rate constants estimated from control and PSC833 in situ perfusion studies shown in Table 3. Solid lines represent the extraction ratio calculated by Equation 3 (Cummins et al., 2001) and dotted lines represent the extraction ratio calculated by Equation 4 (Fisher et al., 1999), which is equal to the model predicted extraction ratio (Equation 5).

FIGURE 1

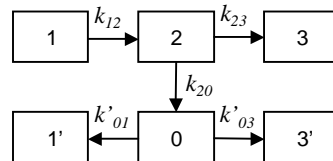


FIGURE 2

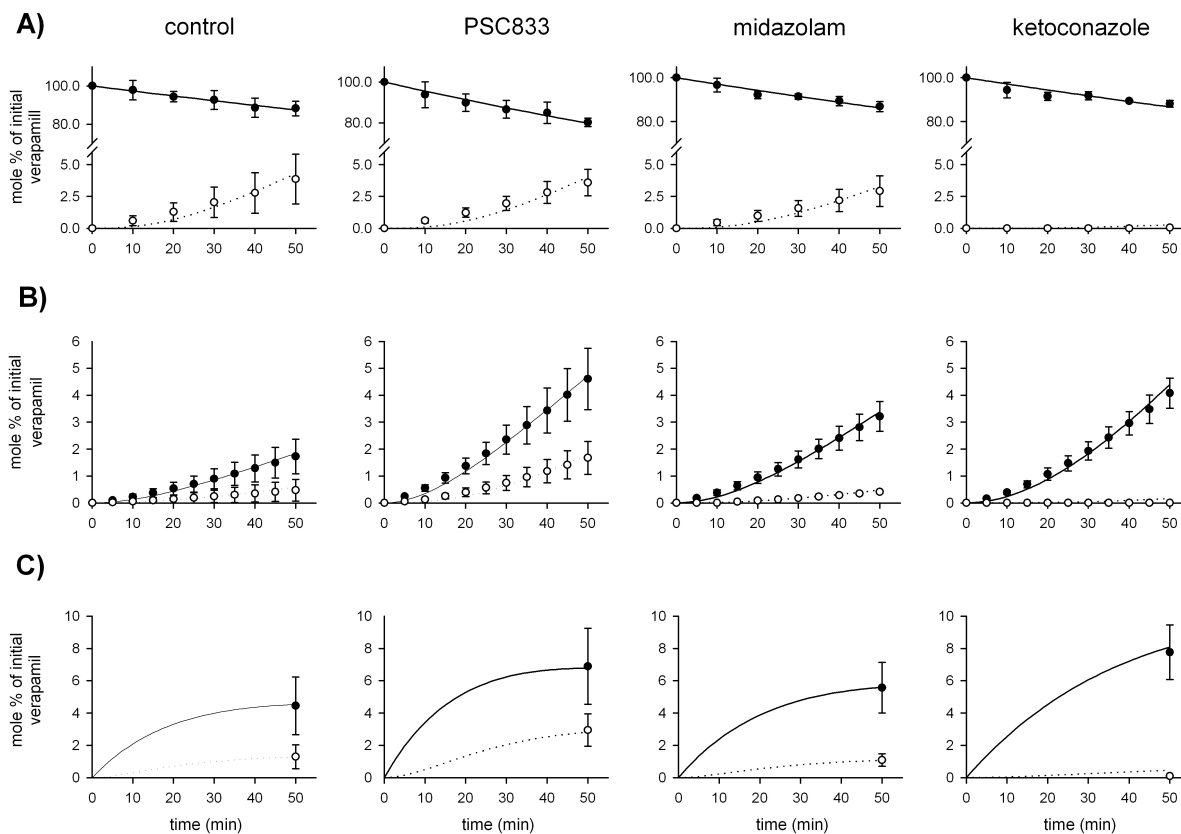


FIGURE 3

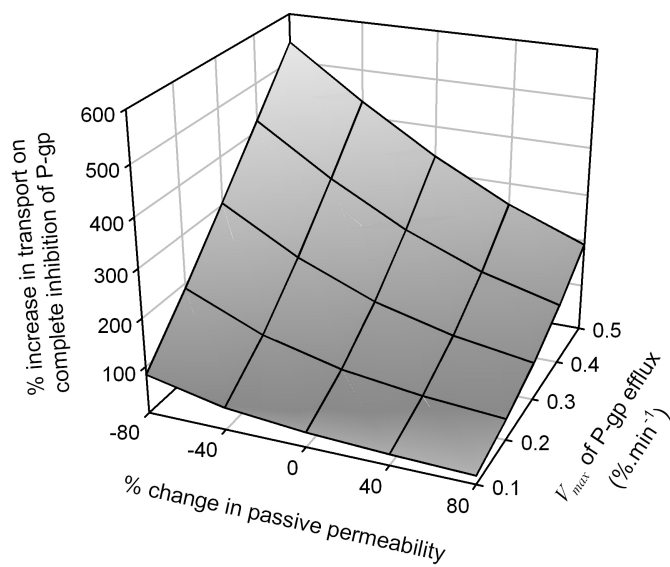


FIGURE 4

